Theory of spontaneous parametric down-conversion from photonic crystals

Anthony N. Vamivakas, Bahaa E. A. Saleh,* Alexander V. Sergienko, and Malvin C. Teich
Quantum Imaging Laboratory,† Departments of Electrical & Computer Engineering and Physics, Boston University, Boston, Massachusetts 02215, USA
(Received 12 May 2004; published 14 October 2004)

An effective-medium approach is used to derive a set of coupled-mode equations describing quadratic parametric interactions in a one-dimensional inhomogeneous medium of finite length. The solutions for both copropagating and counterpropagating interactions are used to study the quantum-mechanical process of spontaneous parametric down-conversion (SPDC). An example is studied in which the inhomogeneous medium is a photonic crystal. The effect that device geometry has on both the efficiency and bandwidth of SPDC is explored. With appropriate design, we find that it is possible not only to enhance the efficiency of SPDC, but also to generate broadband copropagating and narrowband counterpropagating down-converted light. A setup is proposed with the potential to act as a source of entangled photon pairs.

DOI: 10.1103/PhysRevA.70.043810 PACS number(s): 42.50.Dv, 42.65.Ky

I. INTRODUCTION

In homogeneous, nonlinear media, efficient exchange of energy between interacting modes of the electromagnetic field is determined by the linear and nonlinear susceptibilities of the medium. Specifically, the material's permittivity determines how "phase matched" is a given parametric process, whereas the actual coupling of energy between the modes is a function of the material's nonlinear polarizability. In bulk nonlinear optics, the experimenter is ultimately constrained by the linear and nonlinear properties available in existing media.

In an attempt to circumvent material constraints, much work has focused on the possibility of using periodic media to mediate nonlinear processes. The idea of using inhomogeneous media in nonlinear optics, though, is not new. Armstrong *et al.* [1], Franken and Ward [2], and Yariv [3] long ago proposed the introduction of periodic structure into the linear and nonlinear material properties to aid in phase matching parametric interactions. In particular, periodic modulation of the nonlinearity to assist in phase matching nonlinear processes has been coined quasiphase matching (QPM). QPM has been studied in the context of classical and quantum nonlinear optics [4–8]. The introduction of the periodic, nonlinear modulation leads to both flexibility in phase matching and also makes accessible a material's largest nonlinear coefficient. But, even though QPM can allow experimenters to access a material's largest nonlinear coupling coefficient, QPM is still constrained to the material's largest available nonlinear coefficient.

It has only recently been understood that periodic modulation of a nonlinear material's refractive index can lead to enhanced conversion efficiencies in parametric processes [9–12]. By proper selection of the periodic structure's linear properties and physical geometry, it is possible to achieve the phase matching flexibility of QPM while at the same time realize effective nonlinear coupling coefficients larger than any coupling coefficients available from homogeneous nonlinear media [13].

Photonic crystals, structures with the aforementioned periodicity in the medium's linear properties, were first conceived by Yablonovitch and John [14,15]. Initial interest was directed toward determining how such structures could modify the rate of an atom's spontaneous emission or provide a means for localizing electromagnetic radiation. Currently, though, photonic crystals are on the verge of changing how one practices nonlinear optics. Instead of searching handbooks in the hope of finding a homogeneous material with particular physical attributes, a device that possesses the desired properties is engineered.

The enhancement of parametric interactions afforded by photonic crystals has been relatively unexplored in the realm of quantum nonlinear optics [9]. Specifically, the use of a photonic crystal to mediate the process of spontaneous parametric down-conversion (SPDC) would be of interest to the experimental quantum optics community. SPDC acts as a robust source of entangled photon pairs for a variety of experiments, but unfortunately suffers from low conversion efficiencies, on the order of 10^{-9} photon pairs per mode per pump photon [16]. Sources of ultrabright entangled pairs are of current interest and photonic crystals could provide the means for realizing high-flux entangled photon sources [17]. Also, the potential for a photonic crystal acting as a source of broadband entangled photons would be of interest in quantum optical metrology techniques such as quantum optical coherence tomography [18].

In this paper we develop a general theory that describes SPDC from media with a one-dimensional spatial variation in both its linear and nonlinear dielectric functions. We then use this theory to examine the special case in which the material's linear properties are periodic and its nonlinear properties are either periodic or homogeneous. We explore the effect of the device's geometry and material parameters on both the conversion efficiency and spectrum of SPDC. By manipulating these two controls, it is possible to engineer both the spectrum and overall conversion efficiency of SPDC. We find that periodic structures simultaneously sup-

*Email address: besaleh@bu.edu
†URL: http:www.bu.edu/qil

port copropagating and counterpropagating down conversion.

II. SPDC FROM A ONE-DIMENSIONAL INHOMOGENEOUS MEDIUM

A semiclassical approach is sufficient for correctly calculating the efficiency of SPDC from homogeneous, nonlinear media [19,20]. The solutions of the coupled-mode equations governing three-wave mixing processes and knowledge of the quantum nature of the electromagnetic field, when combined, yield the appropriate analytic expression for the SPDC conversion efficiency. However, it is assumed in the aforementioned calculation that the medium's linear and nonlinear susceptibilities are homogeneous. If no assumption is made about the spatial distribution of the linear and nonlinear susceptibilities, then it is necessary to modify the usual three-wave mixing coupled-mode equations in a manner consistent with the inhomogeneous material properties.[1]

For one-dimensional quadratic nonlinear interactions, the following set of scalar Helmholtz equations govern all possible interactions for three field modes with angular frequencies $\omega_p = \omega_s + \omega_i$, where the subscripts p, s, and i denote pump, signal, and idler:

$$\left(\frac{d^2}{dz^2} + \frac{\omega_s^2 \varepsilon_s(z)}{c^2}\right) E_s = \frac{-2\omega_s^2 d(z)}{c^2} E_i^* E_p,$$

$$\left(\frac{d^2}{dz^2} + \frac{\omega_i^2 \varepsilon_i(z)}{c^2}\right) E_i = \frac{-2\omega_i^2 d(z)}{c^2} E_s^* E_p,$$

$$\left(\frac{d^2}{dz^2} + \frac{\omega_p^2 \varepsilon_p(z)}{c^2}\right) E_p = \frac{-2\omega_p^2 d(z)}{c^2} E_s E_i. \tag{2.1}$$

In Eq. (2.1), both the medium's permittivity ε and nonlinear coupling coefficient d are functions of the position z. Also, the subscripts on the permittivity allow for the possibility of material dispersion.

Recently, a generalized coupled-mode theory has been developed to characterize one-dimensional quadratic, nonlinear interactions of linearly polarized monochromatic plane-wave fields in isotropic, dispersive linear gratings with arbitrarily deep index contrast [10]. The approach relies on decomposing the steady-state solution of the linear Helmholtz equation, within the grating, into a superposition of left-to-right (LTR) and right-to-left (RTL) propagating modes. The general solution for the total field $E_m(z)$ at angular frequency ω_m is

$$E_m(z) = A_m^{(+)}(z)\Phi_m^{(+)}(z) + A_m^{(-)}(z)\Phi_m^{(-)}(z), \quad m = s,i,p, \tag{2.2}$$

where $A_m^{(\pm)}(z)$ are the complex envelopes of the electric field incident on the structure from the left(+)/right(−) and $\Phi_m^{(\pm)}(z)$ are the LTR/RTL mode functions. The functions $\Phi_m^{(\pm)}(z)$ can be calculated using the standard linear matrix transfer technique assuming a unit-amplitude field incident from the left to right [21]. The effect of the material's nonlinear polarization is to permit exchange of energy between the LTR-RTL complex envelopes of the field modes at different angular frequencies, provided energy conservation is not violated.

Recognizing that the dynamics governed by Eq. (2.1) occurs on two distinct length scales makes it possible to derive coupled-mode equations governing general three-wave mixing processes in one-dimensional inhomogeneous media. Specifically, we assume the effect of the nonlinear polarizability [the source term in Eq. (2.1)] is to modulate the solution in Eq. (2.2) far more slowly than the rapid variation of the linear solution itself [10]. Physically, the parameters describing the medium vary on a length scale comparable with the amplitude modulation of the linear solution, whereas the variation of each mode's complex envelope due to nonlinear coupling occurs over a much larger distance. This does not mean that the nonlinear coupling coefficient is small in magnitude, but rather that significant energy exchange among the modes requires a length that is far greater than the variation of the medium's parameters. Introducing this physical intuition into our mathematical equations requires the use of a perturbation technique known as a multiple-scale expansion.

As detailed by D'Aguanno *et al.* [10], the multiple-scale expansion leads to the following set of coupled mode equations for copropagating pump, signal, and idler modes of the field in the undepleted pump approximation $[A_p^{(+)}(z) \cong A_p^{(+)}(0)]$:

$$\frac{dA_s^{(+)}}{dz} = -j\omega_s K_s^{\mathrm{co}} A_i^{(+)*}(z),$$

$$\frac{dA_i^{(+)}}{dz} = -j\omega_i K_i^{\mathrm{co}} A_s^{(+)*}(z), \tag{2.3}$$

where

$$K_m^{\mathrm{co}} = Z_0 B_m^{\mathrm{co}} A_p^{(+)}(0), \quad m = s,i, \tag{2.4}$$

$$B_m^{\mathrm{co}} = \frac{p_m^{(-,-)}\Gamma_m^{(+,+)} - p_m^{(+,-)}\Gamma_m^{(-,+)}}{\det(p_m)}, \tag{2.5}$$

$$[p_m]^{(n,k)} = \frac{1}{L}\left(\frac{jc}{\omega_m}\right)\int_0^L \Phi_m^{(n)*}(z)\frac{d}{dz}\Phi_m^{(k)}(z)dz, \quad (n,k) \in \{+,-\}, \tag{2.6}$$

$$\Gamma_s^{(n,k)} = \Gamma_i^{(n,k)} = \frac{1}{L}\int_0^L d^{(2)}(z)\Phi_s^{(n)*}(z)\Phi_i^{(k)*}(z)\Phi_p^{(+)}(z)dz, \quad (n,k) \in \{+,-\}. \tag{2.7}$$

Here, j is the imaginary unit, Z_0 is the impedance of free space and L is the medium length. The superscript "co" signifies copropagating signal and idler modes. The K_m^{co} coefficients are effective, complex coupling coefficients since they are functions of the generally complex LTR/RTL mode pro-

[1]Note that Ref. [7] addresses the case when only the nonlinear polarizability is periodic.

files. Note the absence of an explicit function of the phase mismatch between the interacting modes. The phase matching conditions appear implicitly in the above coupled-mode equations through the effective, complex coupling coefficients K_m^{co}. To ensure efficient parametric processes, $\Phi_m^{(\pm)}$ of the field modes must overlap within the inhomogeneous medium.

Equations (2.3) are the usual equations for a parametric amplifier with a complex coupling coefficient. If we renormalize the field complex envelopes according to $a_m^{(+)} = A_m^{(+)} B_m^{\mathrm{co}}/\omega_m$, then it is possible to symmetrize Eq. (2.3). Specifically

$$\frac{da_s^{(+)}}{dz} = -jg^{\mathrm{co}} a_i^{(+)*}(z),$$

$$\frac{da_i^{(+)}}{dz} = -jg^{\mathrm{co}} a_s^{(+)*}(z), \tag{2.8}$$

where $g^{\mathrm{co}} = \sqrt{\omega_s \omega_i Z_0^2 B_s^{\mathrm{co}} B_i^{\mathrm{co}}}$. The solution for the signal in the absence of any idler input is

$$a_s^{(+)}(z) = -ja_i^{*(+)}(0)\sinh(g^{\mathrm{co}} z). \tag{2.9}$$

At the end of an inhomogeneous medium of length L, assuming low gain ($g^{\mathrm{co}} L \ll 1$), the power P_s^+ in the signal mode will then be

$$P_s^{(+)}(L) = C_s^{\mathrm{co}} \frac{2\pi}{\hbar\omega_i} \frac{L^2}{A} P_i^{(+)}(0) P_p^{(+)}(0), \tag{2.10}$$

where

$$C_s^{\mathrm{co}} = 2\eta_0^3 {\omega_s}^2 |B_s^{\mathrm{co}}|^2 \frac{n_{\mathrm{eff,real}}(\omega_s)}{n_{\mathrm{eff,real}}(\omega_i) n_{\mathrm{eff,real}}(\omega_p)}. \tag{2.11}$$

Here $n_{\mathrm{eff,real}}(\omega_m)$ is the effective index defined for each of the interacting field modes and A is the transverse crystal area. To determine $n_{\mathrm{eff,real}}(\omega_m)$, the effective dispersion relation, we use knowledge of the inhomogeneous structure's *linear* input/output relation and construct an equivalent-length homogeneous medium sharing an identical input/output relation [22].

Focusing on single transverse-mode interactions, it is now possible to derive an expression for the output signal power assuming that the only input idler power is the vacuum noise energy. It is here that we make the "quantum assumption" to derive an expression for the efficiency of SPDC. Specifically, the incremental output power, in the signal mode, due to input pump power and a single quantum of energy in each of the idler modes $d(P_i/A) = 1 \times \hbar\omega_i \times d\omega_i/2\pi$ is

$$dP_s^{(+)}(L) = C_s^{\mathrm{co}} \frac{L^2}{A} P_p^{(+)}(0) d\omega_i. \tag{2.12}$$

The conversion efficiency of pump photons into signal photons is determined by integrating Eq. (2.12) over all idler frequencies

$$\eta_{\mathrm{eff}}^{\mathrm{co}} = \frac{P_s^{(+)}(L)}{P_p^{(+)}(0)} = \frac{L^2}{A} \int C_s^{\mathrm{co}}(\omega_i) d\omega_i, \tag{2.13}$$

where we have made explicit the dependence of C_s^{co} on the idler frequency. Only those idler noise photons that are commensurate with energy and momentum conservation contribute to Eq. (2.13). Also, the spectral width of above integral's kernel gives a measure of the signal mode's bandwidth.

The generalized coupled-mode equations (2.13) describe the interaction of copropagating field modes. The generalized coupled-mode theory also governs the dynamics for other parametric processes. In particular, it is possible to derive an expression analogous to Eq. (2.13) for counterpropagating signal and idler modes. The end result is

$$\eta_{\mathrm{eff}}^{\mathrm{counter}} = \frac{P_s^{(-)}(L)}{P_p^{(+)}(0)} = \frac{L^2}{A} \int C_s^{\mathrm{counter}}(\omega_i) d\omega_i, \tag{2.14}$$

where C_s^{counter} is the same as Eq. (2.11) except that

$$B_s^{\mathrm{counter}} = \frac{-p_s^{(-,+)} \Gamma_s^{(+,+)} + p_s^{(+,+)} \Gamma_s^{(-,+)}}{\det(p_s)}. \tag{2.15}$$

Equations (2.13)–(2.15) provide the central results of this paper. The two relations provide expressions for the conversion efficiency and spectrum of both copropagating and counterpropagating SPDC from media with inhomogeneous linear and nonlinear susceptibilities. Examination of Eqs. (2.13) and (2.14) makes clear that the kernel of each integral, $C_s^{\mathrm{counter}}(\omega_i)$ or $C_s^{\mathrm{co}}(\omega_i)$, determines both the efficiency and spectrum of SPDC. Specifically, the spectrum of SPDC can be obtained by plotting the normalized integrand as a function of frequency. Next, if we sum the correctly weighted kernel across all frequencies, it is possible to quantify the conversion efficiency for SPDC. Our specific interest will be in how $|B_s^{\mathrm{co}}|^2$ or $|B_s^{\mathrm{counter}}|^2$ influences the spectrum and efficiency of SPDC for a device with periodic linear material properties, a one-dimensional photonic crystal. Since $|B_s^{\mathrm{co}}|^2$ and $|B_s^{\mathrm{counter}}|^2$ are functions of both the photonic crystal's linear mode profiles, as determined by the linear Helmholtz equation, and the distribution of the material nonlinearity, device geometry is an important consideration in designing a photonic crystal to mediate SPDC. Through appropriate selection of device geometry, it becomes possible to compensate for the phase mismatch introduced by the material dispersion of the individual device layers and realize conversion efficiencies larger than would be expected from an equivalent length medium with homogeneous linear and nonlinear properties.

Prior to presenting the results of the numerical simulations, it is important to elucidate the distinction between using a photonic crystal to mediate a classical, three-wave mixing process and the process of SPDC. In classical nonlinear optics, the energy-conservation constraint yields a *single* permissible solution for a given three-wave interaction. Since only three field modes are involved in the process, it is possible to design a photonic crystal such that the interacting field modes are tuned to peaks of transmission resonances [23] at the edge of the photonic crystal's band gap. Physically this is desirable since the field mode's energy then be-

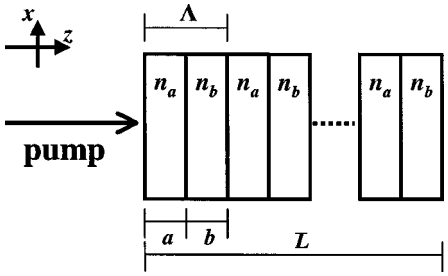

FIG. 1. (a) Schematic of a one-dimensional photonic crystal. The layer of width a has refractive index n_a and the layer of width b layer has refractive index n_b. Also, $n_a=1$ for all frequencies and we assume $n_b(\omega_{s,i})=1.428$ for signal/idler frequencies, but $n_b(\omega_p)=1.519$ for the pump frequency. The field is incident normal to the structure and has either "s" (TE) or "p" (TM) type polarization. Λ is the width of the structure's unit cell and the overall device length is $L=N\Lambda$. In our study, we assume that the field is TE polarized. Initially, the nonlinearity is distributed only in the high index layers and has a value of 44 pm/V in these layers.

comes strongly localized within the structure. Strong localization results in an enhancement of the energy exchange among the modes, provided that the device geometry is selected to compensate for material dispersion so that the interacting modes are phase matched. Mathematically, when the fields are tuned to band-edge resonances and the inhomogeneity is periodic, the significance of the coupling coefficient $|B_s^{co}|^2$ is transparent [10]. It is a simple function of the linear mode profiles and the nonlinear dielectric function.

The discussion provided above should be contrasted with that for the process of SPDC, the inverse process to sum frequency generation. For SPDC, the input of only a pump field mode leads to an *infinite* number of signal and idler mode solutions satisfying the constraint of energy conservation. Design of a photonic crystal to mediate the process of SPDC becomes difficult since the total output SPDC energy is the result of a collective interaction of multiple signal and idler frequency modes. For a given signal and idler pair, the strength of their interaction depends both on how localized each mode is within the structure and how the two down-converted modes overlap with the pump mode. In calculating the overall conversion efficiency of pump power into down-converted photons, there is a tradeoff between the number of contributing modes and how efficiently these modes contribute to SPDC growth. Unfortunately, even though the medium is periodic, $|B_s^{co}|^2$ does not simplify mathematically and its interpretation is less obvious. In the following section we numerically investigate copropagating and counterpropagating SPDC from a one-dimensional photonic crystal.

III. SPDC FROM A ONE-DIMENSIONAL PHOTONIC CRYSTAL

In this section we analyze collinear copropagating and counterpropagating SPDC from a generic one-dimensional photonic crystal. An illustration of the general device we consider is presented in Fig. 1. The material parameters are described in the caption. We assume that the material's linear and nonlinear properties are periodic along the z direction and that the structure has a transverse area A. Further, since we assume the material properties are isotropic and all fields propagate collinearly along z, the structure treats the TE and TM modes identically. Therefore, by focusing initially on type-I SPDC we do not lose any generality in our analysis. Finally, for all studies, the pump mode is assumed to have a wavelength $\lambda_p=845$ nm.

Specifically, we explore the effect device geometry has on both the conversion efficiency per unit length and on the spectrum for copropagating and counterpropagating, collinear SPDC. To study this influence, we designed two generic photonic crystals. The first structure ($S1$) has layer widths of $a=0.25$ μm and $b=0.35$ μm, whereas the second structure ($S2$) has layer widths of $a=0.50$ μm and $b=0.70$ μm. With the layer widths fixed, we then calculated the conversion efficiency per unit length as a function of the number of device periods N. For each structure, the 0-period case corresponds to a single, homogeneous high index layer of length 2.5 μm. The relevance of the 0-period case was to verify that our theory yields the appropriate conversion efficiency when compared with a homogeneous structure.

In Fig. 2, the efficiency per unit length for both copropagating and counterpropagating SPDC is plotted for $S1$. To determine the conversion efficiency we numerically integrated Eqs. (2.13) and (2.14) over all idler angular frequencies. It should be emphasized that by plotting per unit length, the length dependence of the conversion efficiency is removed and it is possible to compare the performance of the photonic crystal structure to a longer, bulk nonlinear crystal. From Fig. 2, it is apparent that by appropriate selection of the number of device periods N, the conversion efficiency of SPDC can be enhanced. In particular, for devices with more than 16 periods, the conversion efficiency per unit length for copropagating SPDC is increased compared to the homogeneous case. Also, for the case of counterpropagating SPDC, the conversion efficiency is enhanced for all numbers N of device periods. $S1$ provided proof-of-principle that enhanced conversion efficiencies are possible from photonic-crystal structures designed with the appropriate number of device periods N. In Fig. 3, we have once again plotted the efficiency per unit length for both copropagating and counterpropagating SPDC, but this time for $S2$. There are two interesting features in this figure. First, for copropagating SPDC, there is an order-of-magnitude enhancement in the SPDC conversion efficiency when compared with a homogeneous nonlinear crystal. By simply doubling the individual layer widths of $S1$, the SPDC conversion efficiency is dramatically affected. Second, in the counterpropagating case, we see that the conversion efficiency saturates and increasing the number of device periods has no further effect on the conversion process.

To understand the origin of this observed enhancement, it is instructive to examine the complex coupling coefficient $\Gamma_s^{(n,k)}$ [Eq. (2.7)]. $\Gamma_s^{(n,k)}$ is a function of both the structure's nonlinear susceptibility and the mode functions for the three interacting modes. It is a measure of the overlap of these four possibly complex functions. It is necessary that the magnitude of the three mode profiles is commensurate within the structure so that the potential exists for efficient energy ex-

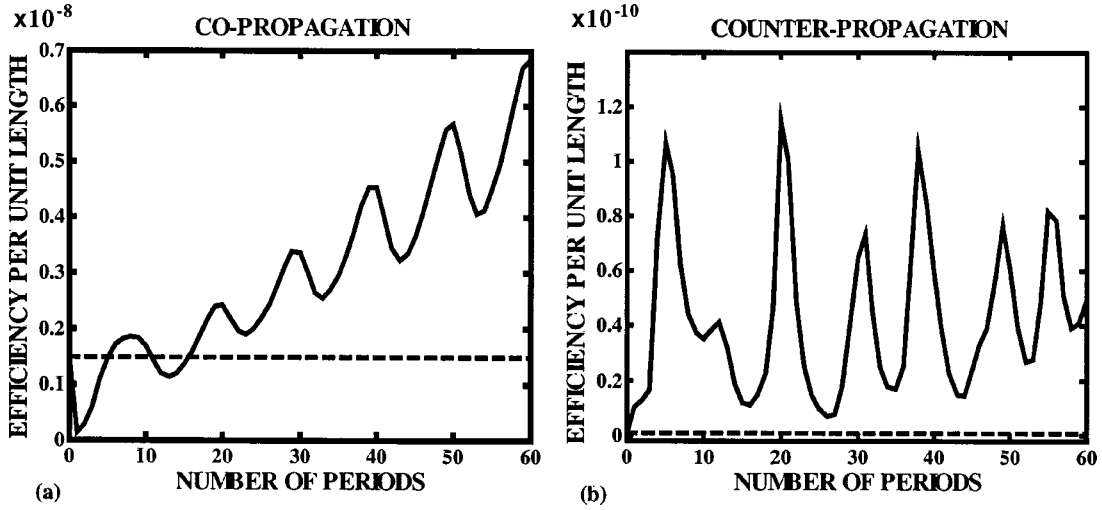

FIG. 2. SPDC efficiency per unit length vs number of device periods N from fixed widths $a=0.25\ \mu\mathrm{m}/b=0.35\ \mu\mathrm{m}$ photonic crystal for (a) copropagating and (b) counterpropagating SPDC. The dashed horizontal line represents the conversion efficiency from a single high-index layer so that the nonlinear crystal is homogeneous. The photonic-crystal material properties are defined in Fig. 1.

change. This alone, though, does not guarantee increased conversion efficiency. Since there is no explicit phase-matching condition, $\Gamma_s^{(n,k)}$ must also ensure that the interacting modes are in phase. If both the previous conditions are satisfied, then it will be possible to mediate nonlinear processes with a photonic crystal. For enhanced conversion efficiencies, it is not only necessary for the previous conditions to be met, but also that the interacting modes are strongly localized within the device. Localization depends on how close a given mode's frequency is to the edge of a band gap. Finally, to understand the influence of the nonlinear distribution on this quantity, we repeated the efficiency calculations reported above, but with a homogeneously distributed nonlinearity of $d^{(2)}=44$ pm/V. This change had no effect on the conversion efficiency. This result is not unexpected since, in both structures considered, the pump mode is tuned to the low-frequency side of a band gap. It is well known that field modes tuned to the low edge of a band gap localize in the material's high-index layers [24]. Therefore, if the pump mode function is zero in the low-index layers, distributing the nonlinearity in these layers will not couple energy from the pump mode into the signal and idler modes.

In the second part of this study, we examined the SPDC spectrum from structures $S1$ and $S2$. To determine the spectrum, for both the copropagating and counterpropagating cases, we evaluated Eqs. (2.13) and (2.14) over all angular frequencies. In Fig. 4 we plot the results of this calculation for both structures. It is clear that manipulation of the device geometry leads to marked differences in the spectral properties of the down-converted photons. First, we see that by changing the number of structure periods, it is possible to realize both degenerate and nondegenerate copropagating and counterpropagating SPDC. In Fig. 4(a), the spectrum is shown for a nine-period $S1$ photonic crystal that exhibits enhanced conversion efficiency when compared to a homogeneous nonlinear crystal. The full width at half maximum

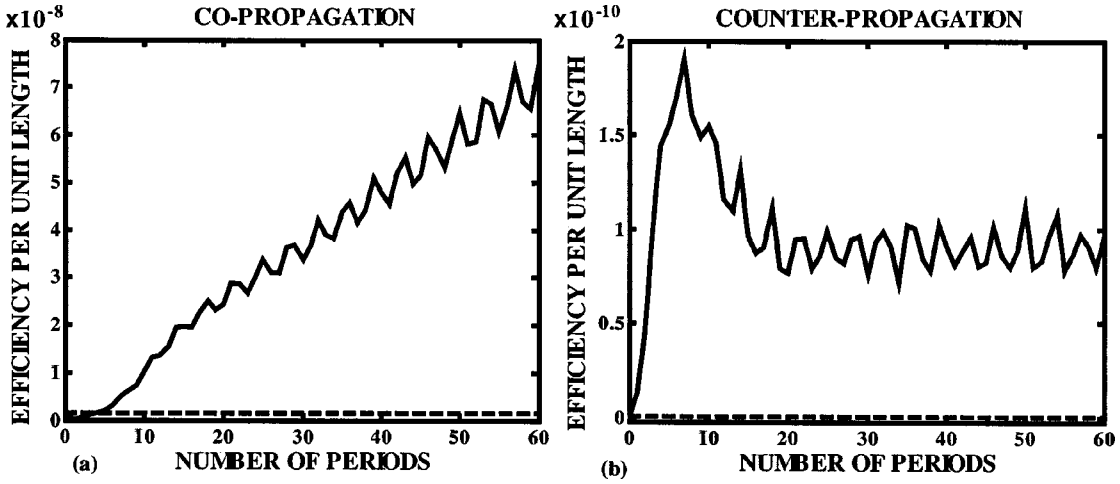

FIG. 3. SPDC efficiency per unit length vs number of device periods N from fixed widths $a=0.5\ \mu\mathrm{m}/b=0.7\ \mu\mathrm{m}$ photonic crystal for (a) copropagating and (b) counterpropagating SPDC. The dashed horizontal line represents the conversion efficiency from a single high-index layer so that the nonlinear crystal is homogeneous. The photonic-crystal material properties are defined in Fig. 1.

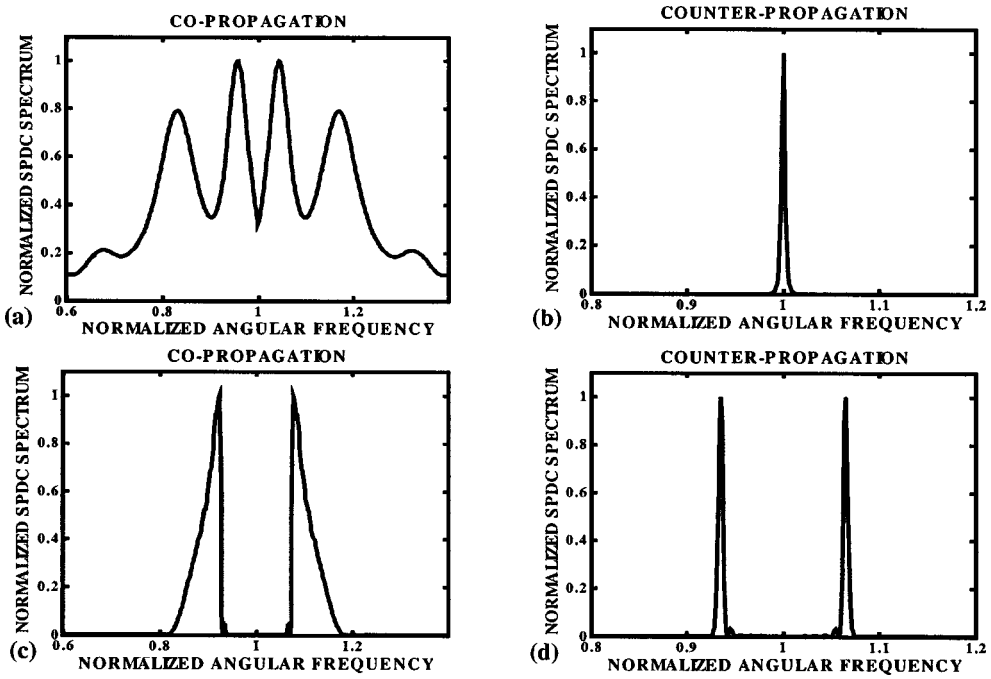

FIG. 4. SPDC spectrum vs frequency normalized to the half the pump mode frequency for (a) copropagating SPDC from a nine-period photonic crystal with $a=0.25\ \mu\mathrm{m}/b=0.35\ \mu\mathrm{m}$, (b) counterpropagating SPDC from a 20-period photonic crystal with $a=0.25\ \mu\mathrm{m}/b=0.35\ \mu\mathrm{m}$; and (c) copropagating, and (d) counterpropagating SPDC from a 50-period photonic crystal with $a=0.5\ \mu\mathrm{m}/b=0.7\ \mu\mathrm{m}$. The photonic-crystal material properties are defined in Fig. 1.

(FWHM) bandwidth for SPDC in this copropagating case is 1.14 μm. One may argue that the reason for such a broad spectrum is the length of $S1$. But, the point is that it may be possible to take advantage of the enhanced conversion efficiency from a photonic crystal and engineer short structures to mediate broadband SPDC at least as efficiently as in a homogeneous nonlinear crystal.

The spectral and spatial features of the counterpropagating SPDC from $S2$, displayed in Fig. 4(d), would be of interest for quantum information processing tasks such as cryptography. With a FWHM bandwidth of 15 nm, the counterpropagating down-converted photons would be in an entangled quantum state. Specifically, by distinguishing between the forward and backward spatial modes, $S2$ would generate discrete frequency entanglement.

It is clear that if one wishes to use a photonic crystal to mediate SPDC, care must be taken in device design. We have given generic examples of how a photonic crystal's geometry and material properties directly influence collinear, copropagating, and counterpropagating SPDC conversion efficiency and spectrum. If the device geometry is chosen such that the interacting modes overlap in phase within the structure, it is possible to overcome the intrinsic device-material dispersion and realize enhanced SPDC conversion efficiencies. At the same time as we observe enhanced efficiency, it is possible to generate both broadband and narrowband SPDC. In particular, we designed a structure that could generate discrete frequency entanglement.

IV. SUMMARY AND CONCLUSIONS

In Sec. II, we developed a general theory to describe spontaneous parametric down conversion from a medium with an inhomogeneous linear and nonlinear dielectric function. In Sec. III, we constrained the inhomogeneity to be periodic and discovered that a photonic crystal simultaneously supports down conversion into copropagating and counterpropagating signal and idler modes. We showed how the device geometry and material parameters directly influence the efficiency and spectrum of the conversion process. Through appropriate design, it is possible to not only achieve enhanced conversion efficiencies, but also to produce degenerate and nondegenerate SPDC with interesting spectral properties.

Recently, there has been much interest within the nonlinear-optics community in using periodically poled (PP) materials as a source of SPDC [5–8]. It is important to compare the use of PP structures with photonic-crystal devices as described here. First, a PP structure is a device that has a periodic nonlinear susceptibility. The length scale of the periodicity is selected depending on the nonlinear process that one is trying to phase match. In particular, a PP nonlinear crystal provides more flexibility in phase matching parametric interactions in comparison to bulk crystals, but the conversion efficiency of such interactions is ultimately constrained by the magnitude of the unpoled crystal's nonlinear coefficient. Also, the types of interactions supported by PP materials are very much influenced by the material properties of the unpoled crystal. From the discussion provided here, it is clear that periodically poling a material allows one to extend the range of operation of the underlying bulk nonlinear crystal.

In contrast, as we have seen, it is possible to utilize a photonic crystal not only to enhance the conversion efficiencies of SPDC, but also to phase match various types of non-

linear interactions. The function of a photonic crystal in mediating SPDC is very much dependent on geometric device properties such as individual layer widths and the number of device periods. The relationship between the underlying crystal's material properties and the periodic photonic crystal is not as clear as it is with the PP structures. In fact, by using photonic crystals, experimenters are no longer ultimately constrained by the underlying bulk crystal material properties, but only by their ingenuity in device design.

Although we have studied a generic structure in this paper, an appropriate choice of semiconductor materials would allow photonic crystals to be realized in practice as a source of down-converted photons. Since our analysis was restricted to a single propagation mode, further study is required to understand the effect that higher-dimensional photonic crystals would have on the down-conversion process. Finally, embedding the photonic-crystal structure in a wave guide would allow the transverse spatial profile of the field mode to be manipulated. The use of a photonic crystal, in conjunction with a wave guiding structure, would give an experimenter total control over the spatial and spectral features of the down-converted photons, as well as the ability to achieve enhanced overall conversion efficiencies not available in bulk nonlinear crystals.

ACKNOWLEDGMENTS

This work was supported by the National Science Foundation; by the Center for Subsurface Sensing and Imaging Systems (CenSSIS), an NSF engineering research center; by the Defense Advanced Research Projects Agency (DARPA); and by the David & Lucile Packard Foundation.

[1] J. A. Armstrong, N. Bloembergen, J. Ducuing, and P. S. Pershan, Phys. Rev. **127**, 1918 (1962).
[2] P. A. Franken and J. F. Ward, Rev. Mod. Phys. **35**, 23 (1963).
[3] A. Yariv, IEEE J. Quantum Electron. **9**, 919 (1973).
[4] M. M. Fejer, G. A. Magel, D. H. Hundt, and R. L. Byer, IEEE J. Quantum Electron. **28**, 2631 (1992).
[5] G. Di Giuseppe, M. Atatüre, M. D. Shaw, A. V. Sergienko, B. E. A. Saleh, and M. C. Teich, Phys. Rev. A **66**, 013801 (2002).
[6] M. C. Booth, M. Atatüre, G. Di Giuseppe, A. V. Sergienko, B. E. A. Saleh, and M. C. Teich, Phys. Rev. A **66**, 023815 (2002).
[7] P. Baldi, M. Sundheimer, K. El Hadi, M. P. de Micheli, and D. B. Ostrowsky, IEEE J. Quantum Electron. **2**, 385 (1996).
[8] G. Kh. Kitaeva and A. N. Penin, JETP **98**, 272 (2004).
[9] K. Sakoda, *Optical Properties of Photonic Crystals* (Springer-Verlag, New York, 2001).
[10] G. D'Aguanno, M. Centini, M. Scalora, C. Sibilia, M. Bertolotti, M. J. Bloemer, and C. M. Bowden, J. Opt. Soc. Am. B **19**, 2111 (2002).
[11] M. Scalora, M. J. Bloemer, A. S. Manka, J. P. Dowling, C. M. Bowden, R. Viswanathan, and J. W. Haus, Phys. Rev. A **56**, 3166 (1997).
[12] A. V. Balakin, V. A. Bushuev, N. I. Koroteev, B. I. Mantsyzov, I. A. Ozheredov, A. P. Shkurinov, D. Boucher, and P. Masselin, Opt. Lett. **24**, 793 (1999).
[13] G. D'Aguanno, M. Centini, M. Scalora, C. Sibilia, Y. Dumeige, P. Vidakovic, J. A. Levenson, M. J. Bloemer, C. M. Bowden, J. W. Haus, and M. Bertolotti, Phys. Rev. E **64**, 016609 (2001).
[14] E. Yablonovitch, Phys. Rev. Lett. **58**, 2059 (1987).
[15] S. John, Phys. Rev. Lett. **58**, 2486 (1987).
[16] L. Mandel and E. Wolf, *Optical Coherence and Quantum Optics* (Cambridge University Press, Cambridge, 1995), Chap. 22.
[17] S. Tanzilli, H. D. Riedmatten, W. Tittel, H. Zbinden, P. Baldi, M. D. Micheli, D. B. Ostrowsky, and N. Gisin, Electron. Lett. **37**, 26 (2001).
[18] A. F. Abouraddy, M. B. Nasr, B. E. A. Saleh, A. V. Sergienko, and M. C. Teich, Phys. Rev. A **65**, 053817 (2002).
[19] D. A. Kleinman, Phys. Rev. **174**, 1027 (1968).
[20] A. Yariv, *Quantum Electronics*, 3rd ed. (Wiley, New York, 1989), Chap. 17.
[21] P. Yeh, *Optical Waves in Layered Media* (Wiley, New York, 1988), Chaps. 1–6.
[22] M. Centini, C. Sibilia, M. Scalora, G. D'Aguanno, M. Bertolotti, M. J. Bloemer, C. M. Bowden, and I. Nefedov, Phys. Rev. E **60**, 4891 (1999).
[23] These transmission resonances coincide with resonances in the density of states of the device.
[24] J. D. Joannopoulos, R. D. Meade, and J. N. Winn, *Photonic Crystals* (Princeton University Press, Princeton, 1995).